THE JOURNAL OF BIOLOGICAL CHEMISTRY VOL. 284, NO. 18, pp. 12384–12398, May 1, 2009

VCP Mutations Causing Frontotemporal Lobar Degeneration Disrupt Localization of TDP-43 and Induce Cell Death*[S]

Received for publication, February 12, 2009 Published, JBC Papers in Press, February 23, 2009, DOI 10.1074/jbc.M900992200

Michael A. Gitcho[‡§], Jeffrey Strider[‡¶], Deborah Carter[‡¶], Lisa Taylor-Reinwald[‡¶], Mark S. Forman[‖], Alison M. Goate[‡§‡‡], and Nigel J. Cairns[‡§¶1]**

*From the [‡]Alzheimer's Disease Research Center and the Departments of [§]Neurology, [¶]Pathology and Immunology, **Psychiatry, and [‡‡]Genetics, Washington University School of Medicine, St. Louis, Missouri 63110 and the [‖]Department of Pathology and Laboratory Medicine, University of Pennsylvania School of Medicine, Philadelphia, Pennsylvania 19104*

Frontotemporal lobar degeneration (FTLD) with inclusion body myopathy and Paget disease of bone is a rare, autosomal dominant disorder caused by mutations in the *VCP* (valosin-containing protein) gene. The disease is characterized neuropathologically by frontal and temporal lobar atrophy, neuron loss and gliosis, and ubiquitin-positive inclusions (FTLD-U), which are distinct from those seen in other sporadic and familial FTLD-U entities. The major component of the ubiquitinated inclusions of FTLD with *VCP* mutation is TDP-43 (TAR DNA-binding protein of 43 kDa). TDP-43 proteinopathy links sporadic amyotrophic lateral sclerosis, sporadic FTLD-U, and most familial forms of FTLD-U. Understanding the relationship between individual gene defects and pathologic TDP-43 will facilitate the characterization of the mechanisms leading to neurodegeneration. Using cell culture models, we have investigated the role of mutant *VCP* in intracellular trafficking, proteasomal function, and cell death and demonstrate that mutations in the *VCP* gene 1) alter localization of TDP-43 between the nucleus and cytosol, 2) decrease proteasome activity, 3) induce endoplasmic reticulum stress, 4) increase markers of apoptosis, and 5) impair cell viability. These results suggest that *VCP* mutation-induced neurodegeneration is mediated by several mechanisms.

Frontotemporal lobar degeneration (FTLD)[2] accounts for 10% of all late onset dementias and is the third most frequent neurodegenerative disease after Alzheimer disease and dementia with Lewy bodies (1). FTLD with ubiquitin-immunoreactive inclusions is genetically, clinically, and neuropathologically heterogeneous (2, 3). FTLD-U comprises several distinct entities, including sporadic forms and familial cases caused by mutations in the genes encoding VCP (valosin-containing protein), GRN (progranulin), CHMP2B (charged multivesicular body protein 2B), TDP-43 (TAR DNA-binding protein of 43 kDa) and an unknown gene linked to chromosome 9 (2, 3). Frontotemporal dementia with inclusion body myopathy and Paget disease of bone is a rare, autosomal dominant disorder caused by mutations in the *VCP* gene located on chromosome 9p13-p12 (4–10) (Fig. 1). This multisystem disease is characterized by progressive muscle weakness and atrophy, increased osteoclastic bone resorption, and early onset frontotemporal dementia, also called FTLD (9, 11). Mutations in *VCP* are also associated with dilatative cardiomyopathy with ubiquitin-positive inclusions (12). Neuropathologic features of FTLD with *VCP* mutation include frontal and temporal lobar atrophy, neuron loss and gliosis, and ubiquitin-positive inclusions (FTLD-U). The majority of aggregates are ubiquitin- and TDP-43-positive neuronal intranuclear inclusions (NIIs); a smaller proportion is made up of TDP-43-immunoreactive dystrophic neurites (DNs) and neuronal cytoplasmic inclusions (NCIs). A small number of inclusions are VCP-immunoreactive (5, 13). Pathologic TDP-43 in inclusions links a spectrum of diseases in which TDP-43 pathology is a primary feature, including FTLD-U, motor neuron disease, including amyotrophic lateral sclerosis, FTLD with motor neuron disease, and inclusion body myopathy and Paget disease of bone, as well as an expanding spectrum of other disorders in which TDP-43 pathology is secondary (14, 15).

TDP-43 proteinopathy in FTLD with *VCP* mutation has a biochemical signature similar to that seen in other sporadic and familial cases of FTLD-U, including sporadic amyotrophic lateral sclerosis, FTLD-motor neuron disease, FTLD with progranulin (*GRN*) mutation, and FTLD linked to chromosome 9p (3, 16). TDP-43 proteinopathy in these disorders is characterized by hyperphosphorylation of TDP-43, ubiquitination, and cleavage to form C-terminal fragments detected only in insoluble brain extracts from affected brain regions (16). Identification of TDP-43 as the major component of the ubiquitin-immunoreactive inclusions of FTLD with *VCP* mutation supports the hypothesis that *VCP* gene mutations cause an alteration of VCP function, leading to TDP-43 proteinopathy.

VCP/p97 (valosin-containing protein) is a member of the AAA (ATPase associated with diverse cellular activities) superfamily. The N-terminal domain of VCP has been shown to be

* This work was supported, in whole or in part, by National Institutes of Health, NIA, Grants P50-AG05681, P01-AG03991, and P30-NS057105. This work was also supported by the Buchanan Fund, the Charles and Joanne Knight Alzheimer Research Initiative, and the Barnes-Jewish Hospital Foundation (St. Louis, MO). A preliminary report of these data was presented (81).

[S] The on-line version of this article (available at http://www.jbc.org) contains supplemental Table 1, Figs. 1–3, and Videos 1 and 2.

[1] To whom correspondence should be addressed: Dept. of Pathology and Immunology, Washington University School of Medicine, Campus Box 8118, 660 S. Euclid Ave., St. Louis, MO 63110. Tel.: 314-362-2386; Fax: 314-362-4096; E-mail: cairns@wustl.edu.

[2] The abbreviations used are: FTLD, frontotemporal lobar degeneration; FTLD-U, FTLD with ubiquitin-positive inclusions; NII, neuronal intranuclear inclusion; DN, dystrophic neurite; NCI, neuronal cytoplasmic inclusion; ER, endoplasmic reticulum; ERAD, ER-associated degradation; PBS, phosphate-buffered saline; CHAPS, 3-[(3-cholamidopropyl)dimethylammonio]-1-propanesulfonic acid; RT, reverse transcription; GAPDH, glyceraldehyde-3-phosphate dehydrogenase.

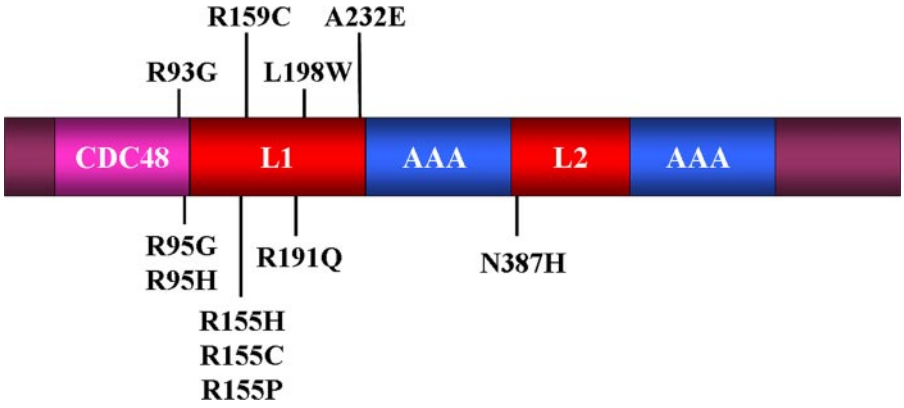

FIGURE 1. **Model of pathogenic mutations and domains in valosin-containing protein.** CDC48 (*magenta*), located within the N terminus (residues 22–108), binds the following cofactors: p47, gp78, and Npl4-Ufd1 (23–25, 28). There are two AAA-ATPase domains (*AAA*; *blue*) at residues 240–283 and 516–569, which are joined by two linker regions (*L1* and *L2*; *red*).

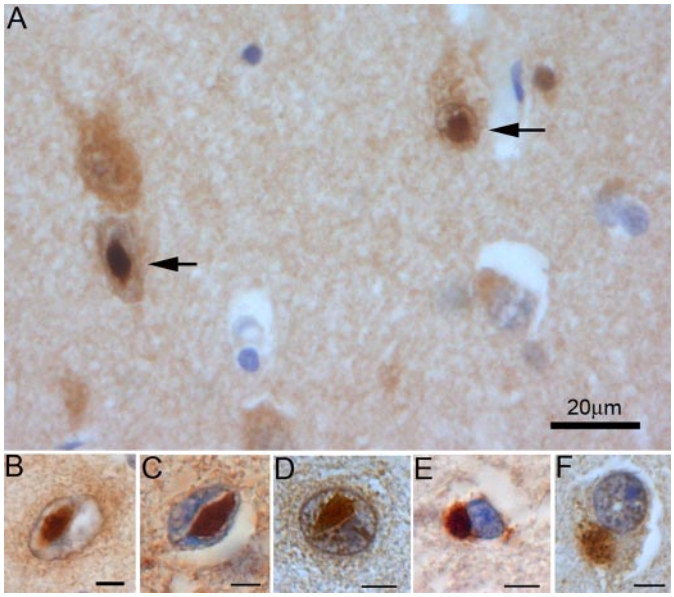

FIGURE 2. **Neuropathology of the brain of a 47-year-old man with frontotemporal lobar degeneration and *VCP* mutation R155H.** *A*, low power micrograph of the superficial laminae of the frontal lobe showing two neurons (*arrows*) containing intranuclear aggregates of VCP. *B*, high power micrograph showing a VCP-immunoreactive intranuclear inclusion. *C*, a TDP-43-immunoreactive intranuclear aggregate. *D*, a ubiquitin-immunoreactive neuronal intranuclear inclusion. *E*, a TDP-43 NCI. *F*, a ubiquitin-immunoreactive NCI. *A* and *B*, VCP immunohistochemistry (*IHC*); *C* and *E*, TDP-43 immunohistochemistry; *D* and *F*, ubiquitin immunohistochemistry. *Scale bar*, 20 μm (*A*) and 5 μm (*B–F*).

involved in cofactor binding (CDC48 (cell division cycle protein 48)) and two AAA-ATPase domains that form a hexameric complex (Fig. 1) (17). Recently, it has been shown that the N-terminal domain of VCP binds phosphoinositides (18, 19). AKT (activated serine-threonine protein kinase) phosphorylates VCP and is required for constitutive VCP function (20, 21). AKT is activated through phospholipid binding and phosphorylation via the phosphoinositide 3-kinase signaling pathway, which is involved in cell survival (22). The lipid binding domain may recruit VCP to the cell membrane where it is phosphorylated by AKT (19).

The diversity of VCP functions is modulated, in part, by a variety of intracellular cofactors, including p47, gp78, and Npl4-Ufd1 (23). Cofactor p47 has been shown to play a role in the maintenance and biogenesis of both the endoplasmic reticulum (ER) and Golgi apparatus (24). The structure of p47 contains a ubiquitin regulatory X domain that binds the N-terminus of VCP, and together they act as a chaperone to deliver membrane fusion machinery to the site of adjacent membranes (25). The function of the p47-VCP complex is dependent upon cell division cycle 2 (CDC2) serine-threonine kinase phosphorylation of p47 (26, 27). Also, VCP has been found to interact with the cytosolic tail of gp78, an ER membrane-spanning E3 ubiquitin ligase that exclusively binds VCP and enhances ER-associated degradation (ERAD) (28). The Npl4-Ufd1-VCP complex is involved in nuclear envelope assembly and targeting of proteins through the ubiquitin-proteasome system (29, 30). The cell survival response of this complex has been found to be important in DNA damage repair though activation by phosphorylation and its recruitment to double-stranded breaks (20, 31). The Npl4-Ufd1-VCP cytosolic complex is also recruited to the ER membrane, interacting with Derlin 1, VCP-interacting membrane proteins (VIMP), and other complexes. At the ER membrane, these misfolded proteins are targeted to the proteasome via ERAD (32–34). VCP also targets IKKβ for ubiquitination to the ubiquitin-proteasome system, implicating VCP in the cell survival pathway and neuroprotection (21, 35–37).

To investigate the mechanism of neurodegeneration caused by *VCP* mutations, we first tested the hypothesis that *VCP* mutations decrease cell viability *in vitro* using a neuroblastoma SHSY-5Y cell line and then investigated cellular pathways that are known to lead to neurodegeneration, including decrease in proteasome activity, caspase-mediated degeneration, and a change in cellular localization of TDP-43.

EXPERIMENTAL PROCEDURES

Tissue Collection and Processing—Human post-mortem brain tissues from clinically and/or neuropathologically well characterized cases were obtained from the Alzheimer's Disease Research Center, Washington University School of Medicine (St. Louis, MO). Brain tissue from the following cases was used: FTLD with the *VCP* R155H mutation, as described previously (13); FTLD with the *GRN* A9D mutation; sporadic FTLD-U; Alzheimer disease ($n = 2$); and two normal aged-matched control cases (see supplemental Table 1 for case descriptions) (7, 13, 16, 38).

Histology and Immunohistochemistry—Paraffin sections from all cases included the frontal lobe (middle frontal gyrus and Brodmann areas 8, 9, and 46), temporal lobe (middle/superior temporal gyrus and Brodmann areas 21 and 22), parahippocampal gyrus, hippocampus, striatum, pons, medulla oblongata, and, when available, spinal cord. Ubiquitin, VCP, and TDP-43 immunohistochemistry was also performed on sec-

tions with disease-representative pathology from cases with other neurodegenerative conditions and normal aged control cases (see supplemental Table 1). Antigen retrieval was performed by microwaving tissue sections in a solution of 0.1 mol/liter citrate buffer, pH 6.0, at 100 °C for 10 min. Immunohistochemistry was undertaken on 7-μm-thick sections prepared from formalin-fixed, paraffin-embedded tissue blocks using the avidin-biotin complex detection system (Vector Laboratories) and the chromagen 3,3-diaminobenzidine; sections were counterstained with hematoxylin, as previously described (3, 13, 16). Antibodies used included those that recognize epitopes of ubiquitin (rabbit polyclonal, 1:1,000; Dako), TDP-43 (rabbit polyclonal, 1:2,000; Proteintech Group, Inc.), and VCP (1:1,000; Abcam). The classification of FTLD-U proposed by the Consortium for Frontotemporal Lobar Degeneration was used because this nosology demonstrates a close correspondence between FTLD-U phenotype and genotype (2, 16, 39). FTLD with *VCP* mutation is distinguished from other FTLD-U subtypes by numerous NIIs and infrequent NCIs and DNs in neocortical areas with relative sparing of the hippocampus, consistent with the pathology previously described in cases with FTLD with *VCP* mutation (13, 16, 40).

Cell Culture and Constructs—Human neuroblastoma cell line SHSY-5Y (ATCC; CRL-226) was plated at ~50% confluency on coverslips in 24-well plates in Iscove's modified Dulbecco's medium and 10% fetal calf serum supplemented with 100 units of penicillin/streptomycin. Retinoic acid (10 μM; Sigma) was used to induce differentiation, activate phosphatidylinositol 3-kinase signaling, and induce phosphorylation of AKT. The proteasome inhibitor MG132 (Calbiochem) was used as a negative control in the proteasome assay, and phosphatidylinositol 3-kinase inhibitor LY294002 (Cell Signaling) inhibits phosphorylation of AKT. The human cytomega-

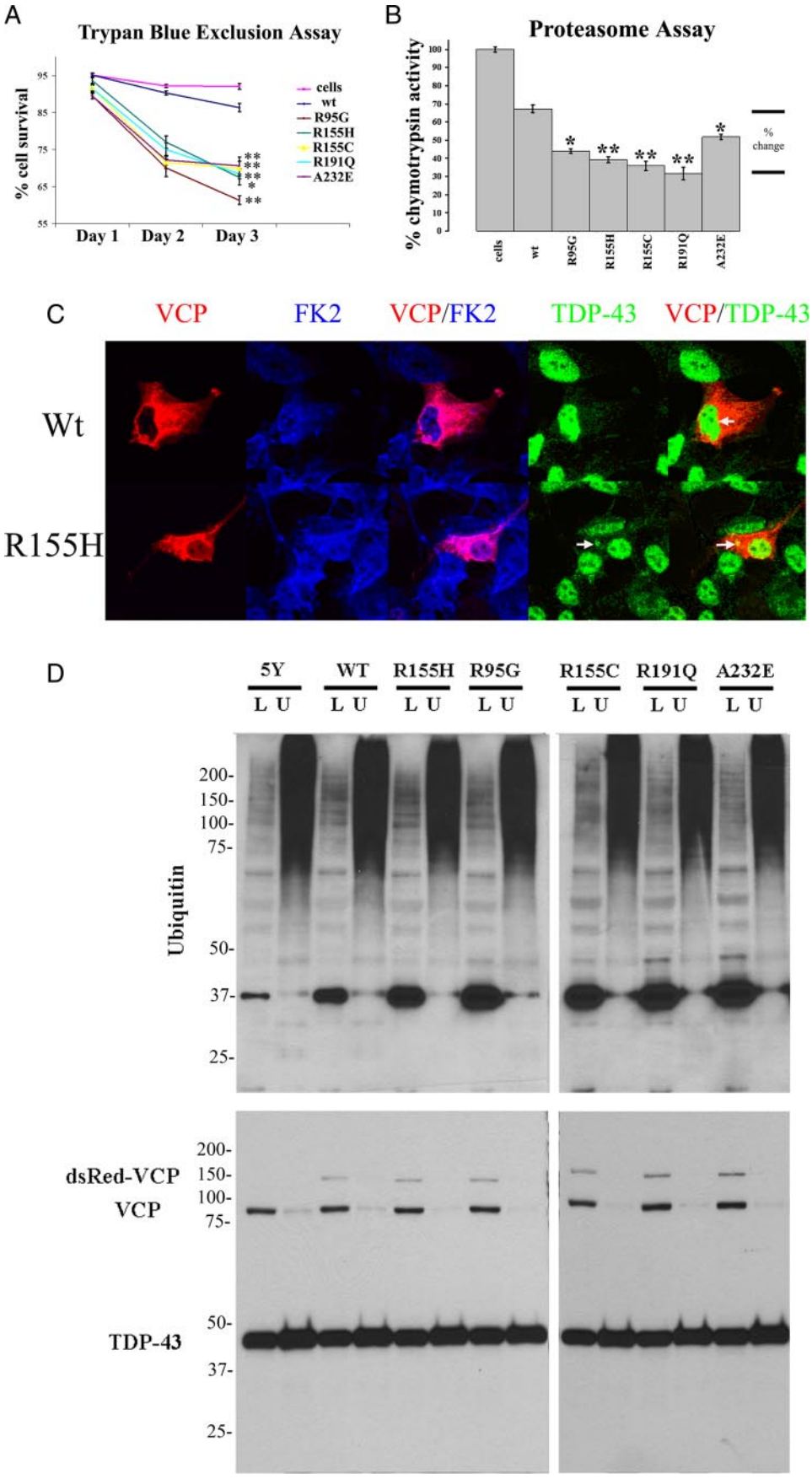

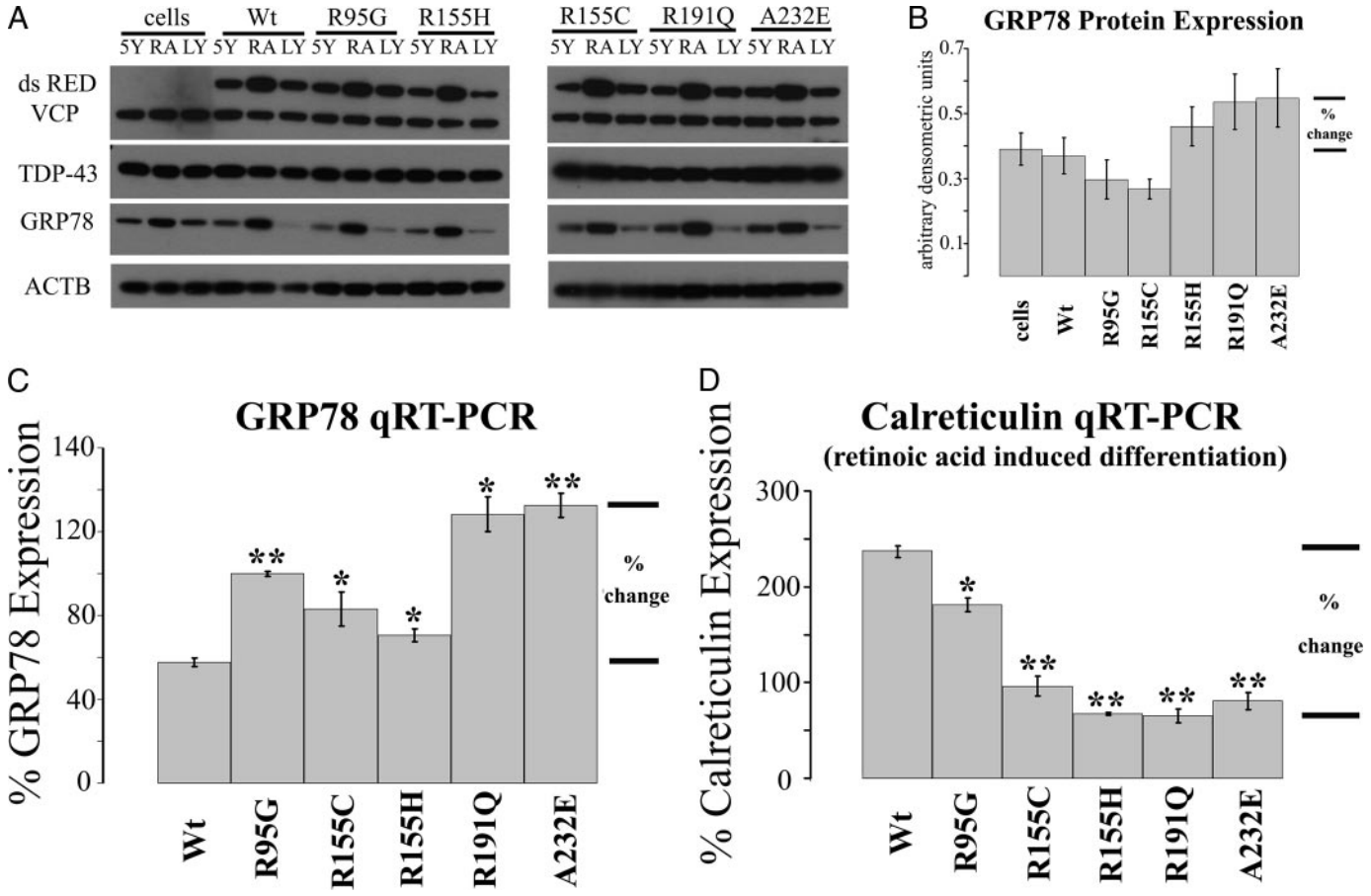

FIGURE 4. **Mutations in *VCP* increase markers of ER stress.** *A*, Western blot analysis of VCP constructs in SHSY-5Y cells under different conditions: untreated SHSY-5Y cells (*5Y*), retinoic acid (*RA*)-induced differentiation, and cells in the presence of phosphatidylinositol 3-kinase inhibitor, LY294002 (*LY*). *B*, there was an increase, but not statistically significant, in GRP78 levels in mutants compared with controls. Values represent relative optical density values of GRP78 in untreated cells in arbitrary units normalized to β-actin (*ACTB*) in three separate experiments. *C*, GRP78 mRNA normalized to GAPDH was significantly increased in mutants, as determined by quantitative RT-PCR (*qRT-PCR*). *D*, quantitative RT-PCR of calreticulin mRNA levels were significantly reduced in mutants compared with WT control when normalized to GAPDH 24 h after transfection and 24 h after retinoic acid-induced differentiation in SHSY-5Y cells. Data are expressed as mean ± S.D.; Student's *t* test; *, $p < 0.05$; **, $p < 0.001$.

lovirus promoter driving N-terminal fusion constructs pDsRed Monomer-C1 (Clontech) (VCP wild type, R155H, R155C, R95G, R191Q, A232E, and the dominant negative E305Q/E578Q mutation) were kindly provided by Dr. Mark Forman (University of Pennsylvania School of Medicine, Philadelphia, PA).

Immunoblotting—Cells were lysed in lysis buffer containing 50 mM Tris-HCl, pH 7.5, 150 mM sodium chloride, 1% Nonidet P-40, 0.5% sodium deoxycholate, 100 μM sodium orthovanadate, and a protease inhibitor mixture (Sigma). Sample concentrations were determined to ensure equal loading, placed in Laemmli sample buffer containing β-mercaptoethanol, and denatured at 100 °C for 5 min. Proteins were separated on a 4–20% SDS-PAGE Tris-glycine gel (Invitrogen), transferred to polyvinylidene difluoride membrane (Millipore), and blocked in 5% instant milk Tris-buffered saline with 0.1% Tween for 1 h. For immunoblotting, primary antibodies were incubated overnight at 4 °C, 1:1000 anti-actin (Abcam), 1:1500 anti-TDP-43 (Proteintech Group, Inc. and Abnova), 1:1000 anti-VCP, 1:1000 BiP/GRP78, 1:1000 AKT, and 1:1000 anti-AKT^{Ser473} (Cell Signaling). Secondary antibodies were incubated for 1 h at room temperature, washed, and exposed to film as previously described (41).

Immunoprecipitation—Cells were lysed in immunoprecipitation buffer containing 50 mM Tris-HCl, pH 7.5, 150 mM sodium chloride, 1% Nonidet P40, 0.5% sodium deoxycholate, 100 μM sodium orthovanadate, and a protease inhibitor mixture (Sigma) and then sonicated briefly on ice. The remaining steps were performed at 4 °C. Lysates from cells were then centrifuged at 10,000 × *g* for 10 min. Supernatant from SHSY-5Y

FIGURE 3. **Mutations in *VCP* decrease cell viability and proteasome activity and increase the amount of soluble ubiquitin in neuroblastoma, SHSY-5Y, cells.** *A*, trypan blue exclusion assay measured cell viability over a 3-day time course after transfection in three separate experiments. The *graph* shows viability of WT compared with mutant *VCP* transiently transfected SHSY-5Y cells ($n = 3$; *, $p < 0.05$; **, $p < 0.001$). *B*, proteasome chymotrypsin cleavage activity in retinoic acid induced differentiated SHSY-5Y cells transiently transfected with VCP constructs assessed 24 h post-transfection ($n = 6$; *, $p < 0.05$; **, $p < 0.001$). *C*, SHSY-5Y cells transiently transfected with monomeric dsRED-VCP constructs; *arrows* indicate colocalization of TDP-43/VCP (*yellow*) and visualization by confocal microscopy (VCP dsRED fusion constructs (*red*), anti-FK2 (*blue*), and anti-TDP-43 (*green*)). *D* (*top*), immunoblotting of low salt and urea-soluble cell fractions reveals a distinct ubiquitin-positive band of ~37 kDa. Soluble low salt (*L*) and soluble urea (*U*) fractions are shown. *5Y*, control SHSY-5Y cells not transfected. *Top*, blot probed with anti-ubiquitin antibodies. *D* (*bottom*), fractions were probed with anti-VCP and anti-TDP-43 antibodies. A single band of ~43 kDa of TDP-43 was identified; no other bands and no cleavage products were detected in the cellular protein fractions. VCP was detected using anti-VCP antibodies, and two bands were identified: full-length VCP of ~97 kDa and VCP-dsRED fusion protein of ~150 kDa.

cells, high salt fractions from human brain were incubated on an orbital shaker with 50 μl of Protein A-agarose beads (Roche Applied Science) for 2–3 h to reduce nonspecific protein binding. Beads were pelleted for 20 s at 10,000 × *g*, and supernatant was placed in a fresh tube with 4 μl of anti-TDP-43- (Proteintech Group or Abnova) or anti-VCP-antibodies (Cell Signaling) overnight. 50 μl of Protein A-agarose beads were then added and allowed to incubate on a rocker for 2 h. Protein A-agarose antibody complexes were pelleted at 10,000 × g for 20 s, and the supernatant was discarded. Beads were washed twice in 500 μl of high salt buffer, 50 mM Tris-HCl, pH 7.5, 500 mM sodium chloride, 0.1% Nonidet P-40, 0.05% sodium deoxycholate, and then washed twice in low salt buffer, 50 mM Tris-HCl, pH 7.5, 0.1% Nonidet P40, 0.05% sodium deoxycholate. Protein A-agarose antibody complexes were resuspended in loading buffer. SDS-PAGE was performed, and proteins were transferred to polyvinylidene difluoride membrane for immunoblotting (see above).

Immunofluorescence Microscopy—Neuroblastoma SHSY-5Y cells were plated at ~50–75% confluency in media on 0.1% gelatin- or poly-D-lysine-pretreated coverslips. After cells adhered, all constructs were transfected following the manufacturer's protocol (Lipofectamine 2000; Invitrogen). At 24, 48, and/or 72 h post-transfection, cells were treated as described, washed in PBS, pH 7.4, three times, and fixed in a 4% paraformaldehyde PBS solution for 20 min. After fixation, cells were washed three times in PBS and blocked for 30 min at room temperature in blocking buffer, 1× PBS, 5% bovine serum albumin, and 0.3% Triton X-100. Primary antibodies were diluted in blocking buffer: Golgi marker, anti-giantin (GOLGB1) (1:2000) (Covance Research Products); anti-TDP-43 (1:500) (Proteintech Group); protein-disulfide isomerase (1:500) (Stressgen), and FK2, which recognizes anti-Lys^{29}-, Lys^{48}-, and Lys^{63}-linked polyubiquitinylated and monoubiquitinylated protein epitopes) at 1:1000 (BioMol) for 1 h. Cells were washed three times in PBS and incubated with Alexa Fluor (λ_{ex} = 488 nm, 543 nm, and/or 633 nm; Invitrogen) fluorescently labeled secondary antibodies in blocking buffer for 1 h, washed three times in PBS, and either mounted directly or incubated with the nuclear marker TOPRO-3 (1:1000) (Invitrogen) for 5 min and then washed three times in PBS. Cells were mounted on slides for confocal microscopy (Prolong Gold; Invitrogen). Images were acquired using a LSM510 Meta laser-scanning confocal microscope (Carl Zeiss Inc., Thornwood, NY) equipped with argon (λ_{ex} = 488 nm), HeNe1 (λ_{ex} = 543 nm), and HeNe2 (λ_{ex} = 633 nm) lasers. A ×63, 1.4 numerical aperture Zeiss Plan Apochromat oil objective was used. Confocal Z slices of 0.5 μm were obtained using the Zeiss LSM510 software (courtesy of Wandy Beatty; Molecular Microbiology Imaging Facility, Washington University).

Cell Death Assay—In order to evaluate cell viability, a trypan blue exclusion assay was performed as previously described (42). Cell counts were determined in triplicate from three separate experiments in four separate fields for transiently transfected SHSY-5Y cells over a 4-day period starting 24 h after transfection.

Caspase Activity Assays—Colorimetric substrates Ac-Asp-Glu-Val-Asp-*p*-nitroaniline (catalog number P-412; Biomol)

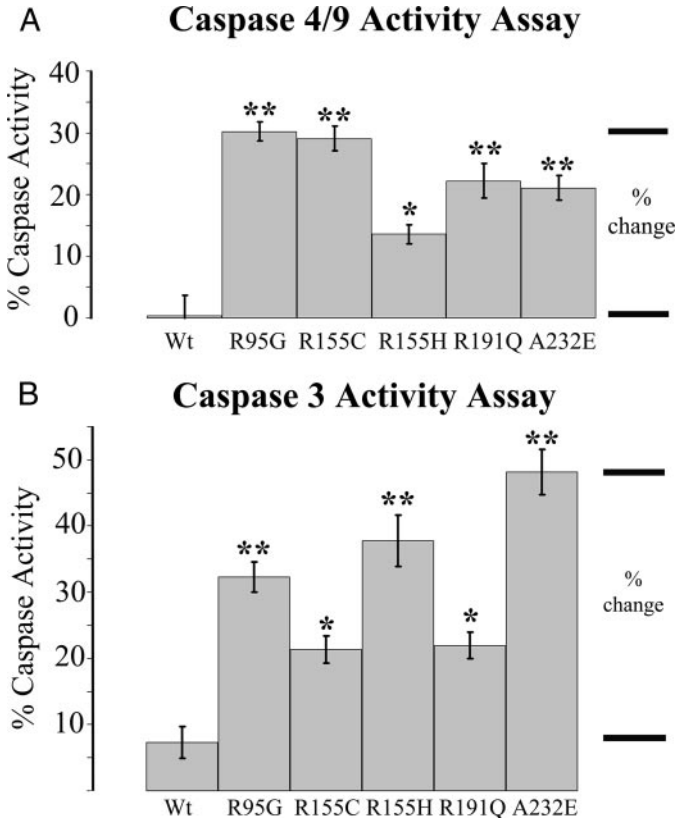

FIGURE 5. **Apoptotic markers are elevated in mutant cell lines compared with controls.** *A*, caspase-4 and/or -9 activity was significantly increased in all mutants. *B*, caspase-3 activity was also elevated in all mutants compared with WT control cells. Transiently transfected overexpressed WT VCP was compared with mutant *VCP* in SHSY-5Y cells (n = 10; *, $p < 0.05$; **, $p < 0.001$).

and Ac-Leu-Glu-His-Asp-*p*-nitroaniline (catalog number PNA154; MP Biomedicals) were used to determine caspase-3/7 activity and caspase-9/4 activity, respectively. Cells were lysed 24 h after transfection in 50 mM HEPES, 100 mM NaCl, 0.1% CHAPS, 0.1 mM EDTA, pH 7.4, lysis buffer, and 50 μg of protein was incubated with 100 μl of 200 μM substrate in 50 mM HEPES, 100 mM NaCl, 0.1% CHAPS, 10 mM dithiothreitol, 0.1 mM EDTA, pH 7.4, in 96-well plates at 37 °C for 24 h. The absorbance of the cleaved product was measured at 405 nm in a microplate reader (Bio-Rad).

Proteasome Activity Assay—Cells were plated at ~50% confluence and transfected with Lipofectamine 2000 (Invitrogen) as described above. After 24 h, cells were rinsed in PBS twice; suspended in 300 μl of lysis buffer containing 10 mM Tris-HCl, pH 7.5, 1 mM EDTA, 2 mM ATP, 4 mM dithiothreitol, 20% glycerol; and sonicated on ice. Lysates were centrifuged at 13,000 × *g* for 10 min at 4 °C, supernatant was removed, and protein concentration was assayed (Coomassie Plus; Pierce). A total of 2.5 μg of protein was loaded per well at a concentration of 0.1 μg/μl with 25 μl of 2× proteasome assay buffer containing 50 mM Tris-HCl, pH 8.8, 0.5 mM EDTA, 40 μM *N*-succinyl-Leu-Leu-Val-Tyr-7-amido-4-methyl-coumain (catalog number S-6510; Sigma), and 40 μM 7-amino-4-methylcoumarin (A989; Sigma). Standards (total of 50 μl in 1× proteasome assay buffer) and a negative control containing 100 μM MG-132 were incubated for 1 h at 37 °C. The reaction was stopped by the

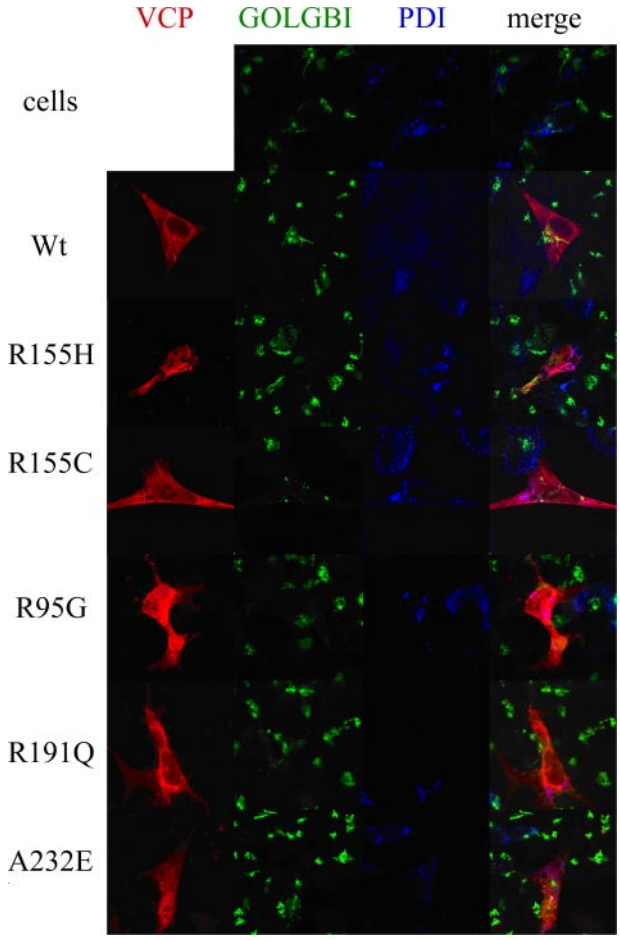

FIGURE 6. **VCP colocalizes with the ER-Golgi network.** Overexpressed dsRED-VCP fusion protein (*red*), GOLGB1 (anti-giantin, *trans*-Golgi) (*green*), and protein-disulfide isomerase (*PDI*; ER marker, secondary; *blue*) were visualized by confocal microscopy.

addition of 250 μl of ice-cold distilled H_2O and assayed immediately on a fluorescent plate reader (λ_{ex} = 380 nm and λ_{em} = 440 nm) (43–45).

Quantitative Real Time RT-PCR and cDNA Synthesis—RNA was isolated from SHSY-5Y cells (RNA Easy; Qiagen) and cDNA synthesis (High Capacity cDNA archive kit; Applied Biosystems). RT-PCR was performed using a 20-μl total reaction with SYBR Green I 2× master mix (Applied Biosystems) with 20 μM gene-specific primers and 2 μl of a 1:40 and 1:80 dilution of cDNA template. An ABI Prism 7900HT real time RT-PCR system (Applied Biosystems) was used for PCR amplification. The efficiency of each PCR was determined by six serial dilutions undertaken in duplicate and repeated three times for SHSY-5Y cDNA, and each expression ratio was based upon normalization with glyceraldehyde-3-phosphate dehydrogenase (GAPDH) cDNA (46). Sequences of real time primers used were as follows: GAPDH-F, TGGAAGGACTCATGACCACAGT; GAPDH-R, GGGCCATCCACAGTCTTCTG; GRP78-F, ACCAATTATCAGCAAACTCTATGGAA, GRP78-R, CATCTTTTTCTGCTGTATCCTCTTCA; CALR-F, TTTGACAACTTCCTCATCACCAA; CALR-R, CCACGTCTCGTTGCCAAAC. The use of GAPDH and β-actin in differentiating neurons has been previously evaluated (47–49).

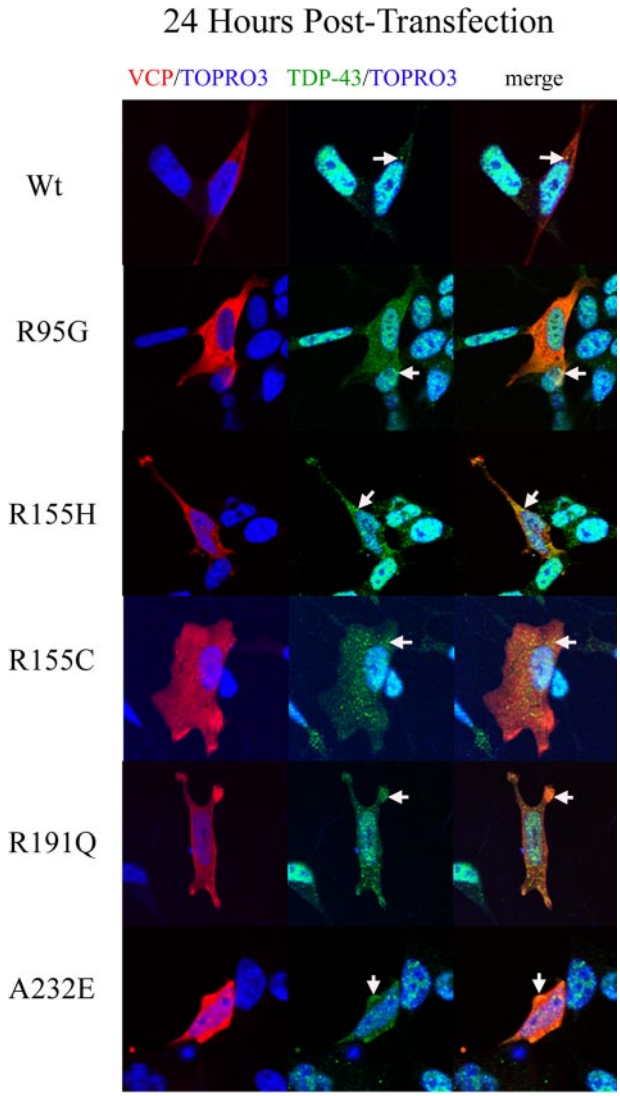

FIGURE 7. **Mutant *VCP* alters endogenous TDP-43 localization 24 h post-transfection.** At 24 h post-transfection, dsRED-VCP fusion protein (*red*), TDP-43 (*green*), and TOPRO-3 (nuclear marker; *blue*) were visualized by confocal microscopy (*arrows* indicate TDP-43 and VCP colocalization and accumulation (*merge/yellow*)).

Statistical Analysis—Data analyses were performed using a repeated measure one-way analysis of variance. For each experiment, the significance levels were determined and data expressed as mean ± S.D.

RESULTS

Inclusions of FTLD with VCP R155H Mutation Contain Ubiquitinated TDP-43 as a Major Component and VCP as a Minor Component—Immunohistochemistry using anti-ubiquitin and anti-TDP-43 antibodies produced similar findings, including a spectrum of neuronal inclusions (NCIs, DNs, and NIIs) (Fig. 2). All NCIs, DNs, and NIIs that were ubiquitin-immunoreactive were also TDP-43-positive; a minority of inclusions was VCP-immunoreactive. Unlike cases of FTLD with *GRN* mutation, where NCIs and DNs are numerous and NIIs much less frequent, in FTLD-U with *VCP* mutation, the most frequent pathological inclusion was the NII, a morphological feature that distinguishes this FTLD-U from other sub-

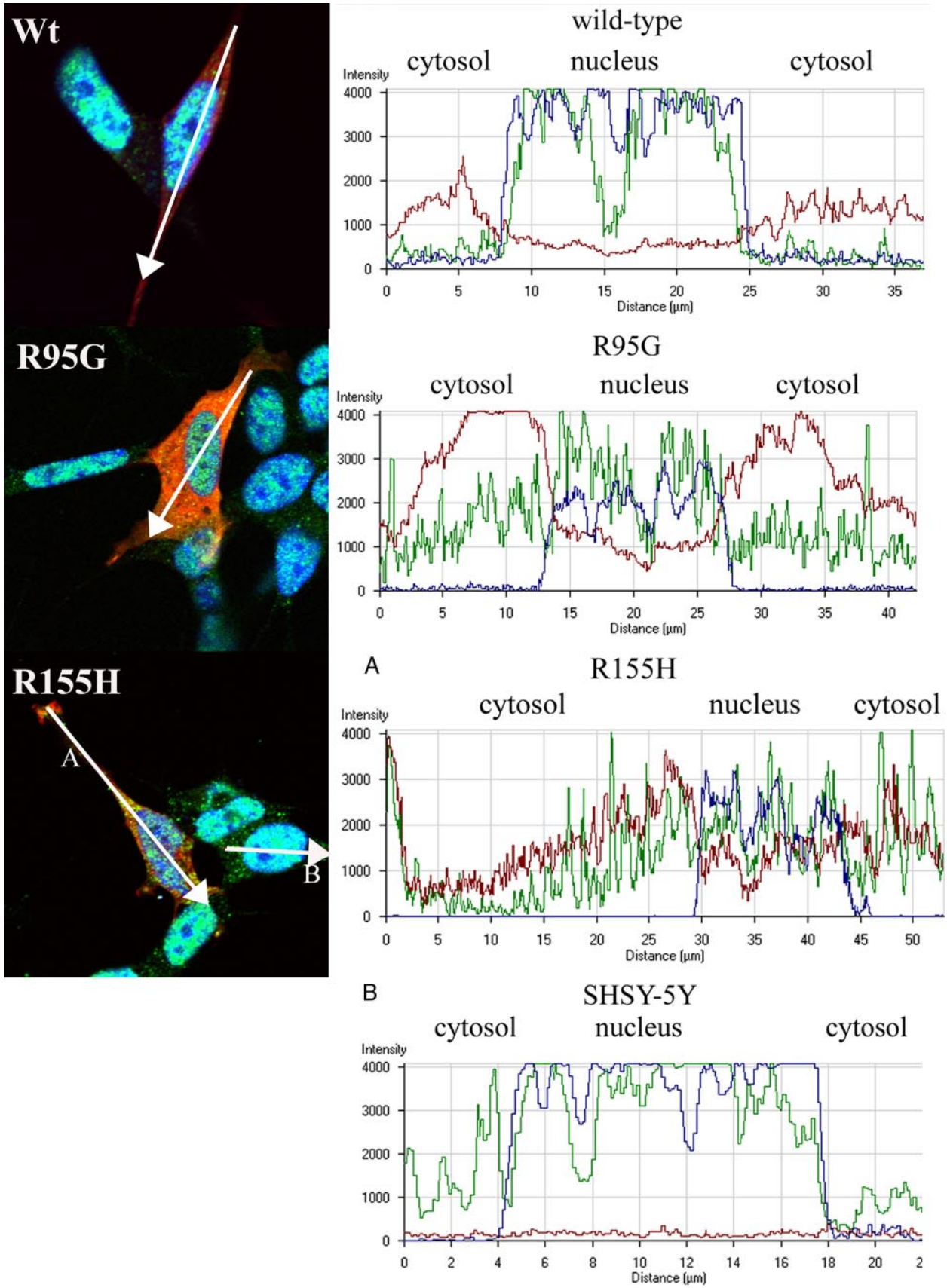

FIGURE 8. **Mutant VCP localizes to the nucleus from cytoplasm 24 h post-transfection.** Wild-type VCP shows no change in cytosolic distribution. R95G and R155H showed a similar spatial pattern of protein localization; the *graphs* show the intensity distribution profile of dsRED-VCP (*red line*), TDP-43 (*green line*), and TOPRO-3, nuclear marker (*blue line*) of the merged image. Intensity profile of R155H (*A*) and control, nontransfected cell (*SHSY-5Y*) profile are represented in the graph (*B*) and show predominantly nuclear and subtle TDP-43 cytoplasmic staining.

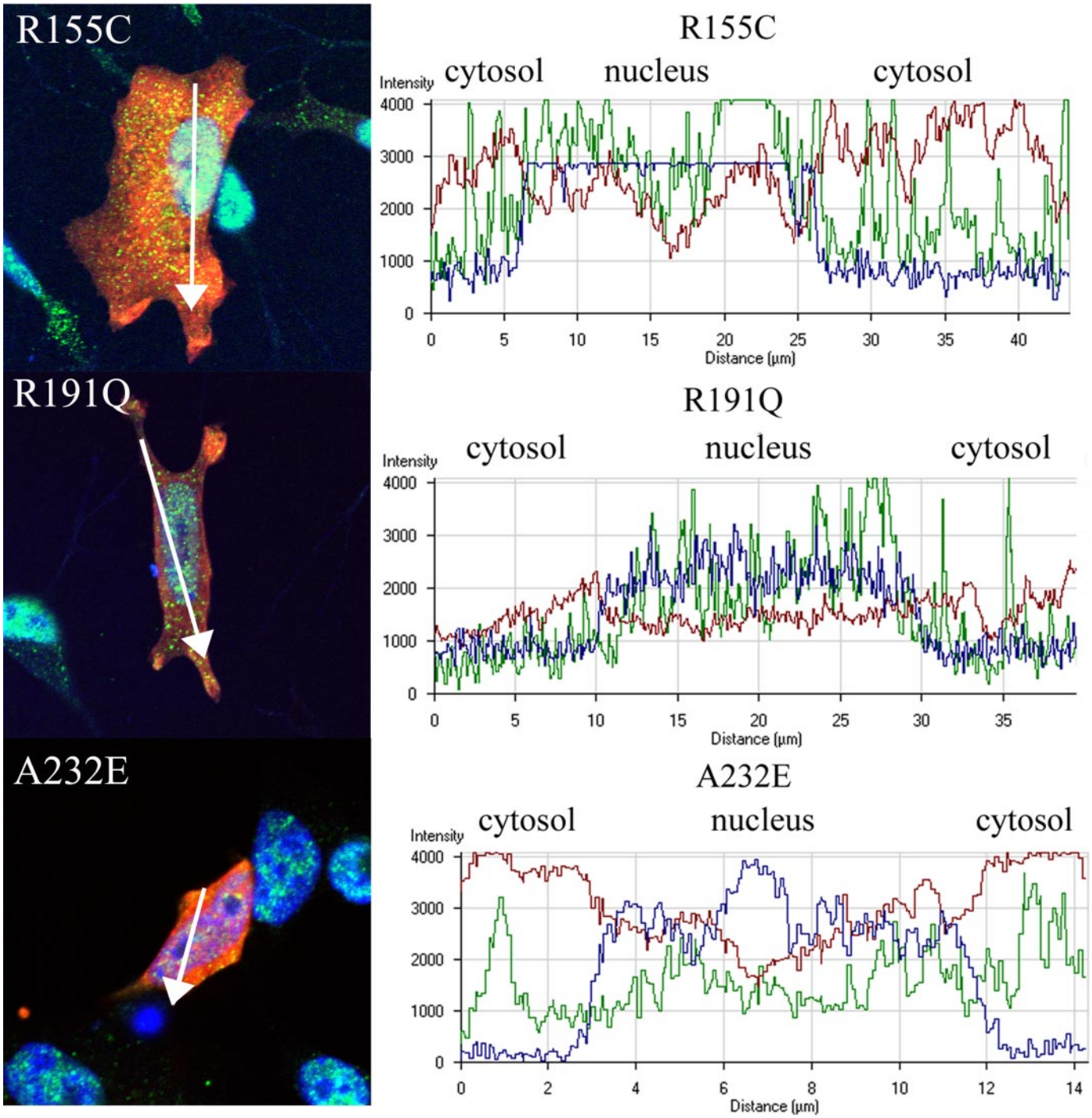

FIGURE 9. **Mutant VCP translocates to the nucleus from the cytoplasm.** VCP translocates to the nucleus and TDP-43 appears more abundant in the cytoplasm of R155C-, R191Q-, and A232E-transfected cells. The *graphs* show the intensity distribution profile of dsRED-VCP (*red line*), TDP-43 (*green line*), and TOPRO-3 (nuclear marker; *blue line*) in the analyzed cells.

types, as previously described (13, 40). These and our previous immunohistochemical and biochemical data indicate that TDP-43 proteinopathy is a signature feature of FTLD with *VCP* mutation (13, 17).

Mutations in VCP Induce Cell Death—To determine the effects on cell viability of overexpressed wild-type (WT) and mutant *VCP* in neuroblastoma cells, we used the trypan blue exclusion assay for evaluating cell viability starting 24 h post-transfection (Fig. 3*A*). All disease-related *VCP* mutations caused a significant decrease in cell viability at 48 and 72 h post-transfection (R95G, 20.2 ± 2.0% ($p < 0.001$); R155H, 13.0 ± 1.2% ($p < 0.05$); R155C, 18.8 ± 1.0% ($p < 0.001$); R191Q, 15.3 ± 1.4% ($p < 0.001$); A232E, 18.2 ± 2.3% ($p < 0.001$) when compared with WT; means were calculated from three separate experiments).

Proteasome Activity Is Impaired by Mutations in VCP—Since cell viability was reduced with mutant *VCP*, and because VCP has previously been shown to be involved in the transport of

misfolded proteins to the proteasome, we next tested whether mutations in *VCP* affected proteasome activity (32). Proteasome activity was measured 24 h post-transfection by cleavage of *N*-succinyl-Leu-Leu-Val-Tyr-7-amido-4-methyl-coumain for chymotrypsin-like activity (Fig. 3*B*). We observed a 32.8 ± 1.5% ($p < 0.001$) decrease in proteasome activity in cells overexpressing WT *VCP* compared with nontransfected cells or vehicle. There was also a significant decrease in proteasome activity in *VCP* mutants compared with WT: R95G, 23.2 ± 2.6% ($p < 0.05$); R155H, 27.7 ± 1.3% ($p < 0.001$); R155C, 31.4 ± 1.6% ($p < 0.001$); R191Q, 35.6 ± 3.5% ($p < 0.001$); A232E, 15.4 ± 1.5% ($p < 0.05$) (means were calculated from three separate experiments). Since ubiquitin-positive inclusions were observed in post-mortem brain (Fig. 2) and mutations in *VCP* with defects in ERAD have been shown to cause an increase in polyubiquitinated aggregates in muscle, we tested whether these aggregates were present in our tissue culture model (50). There was no apparent increase in the relative amount of FK2 (specific for mono- and polyubiquitin protein conjugates) in the R155H mutant compared with WT cells (Fig. 3*C*), but we did observe that VCP and FK2 had more robust colocalization in R155H than WT-transfected cells (Fig. 3*C*; for mutant *VCP* and TDP-43 and FK2 colocalization, see supplemental Fig. 1). Interestingly, in WT-expressing cells, TDP-43 and VCP were observed in proximity to the ER/nuclear envelope (Fig. 3*C*) in both mutant and WT *VCP* in 60% of transfected cells (Fig. 3*C*). In R155H and other mutant *VCP*-expressing cells, there were punctate cytosolic TDP-43/VCP-positive aggregates (Fig. 3*C*). This colocalization in the neuroblastoma cell line is reminiscent of that observed in the pathological inclusions of FTLD-U with *VCP* mutation (Fig. 2, *C–F*).

Sequentially fractionated post-mortem brain tissue from amyotrophic lateral sclerosis and FTLD with TDP-43 proteinopathy displays a unique biochemical signature: hyperphosphorylated TDP-43, an increase in ubiquitinated protein aggregates, and cleaved C-terminal fragments (15). To determine whether our tissue culture system displayed this biochemical signature, we took soluble low salt and urea fractions of SHSY-5Y cells and analyzed these fractions by Western blot (Fig. 3*D*). In the soluble fractions, there was a relative increase in the amount of ubiquitinated proteins compared with WT and untransfected cells (Fig. 3, *D* and *F*). Although we did not detect a 47 kDa band or a 25-kDa cleavage product, as has been reported in FTLD-U and amyotrophic lateral sclerosis brain, there was a distinct ubiquitin-positive band of ~37 kDa that is most likely a covalently linked ubiquitin tetramer that increased in the mutant-expressing cells, consequent to a decrease in proteasome activity (Fig. 3*B*). We found no increase in the quantity of ubiquitinated proteins in the insoluble fractions of SHSY-5Y cells expressing mutant *VCP* (Fig. 3*D*). Unlike in human disease, we were unable to detect any hyperphosphorylated or cleaved TDP-43 in either fraction in the transfected overexpressed mutant *VCP* (Fig. 3*D*) in neuroblastoma cells.

Since VCP contributes to ERAD function and a decrease in proteasome activity has been shown to increase ER stress and the unfolded protein response, we investigated whether mutations in *VCP* cause an increase in ER stress (50–52).

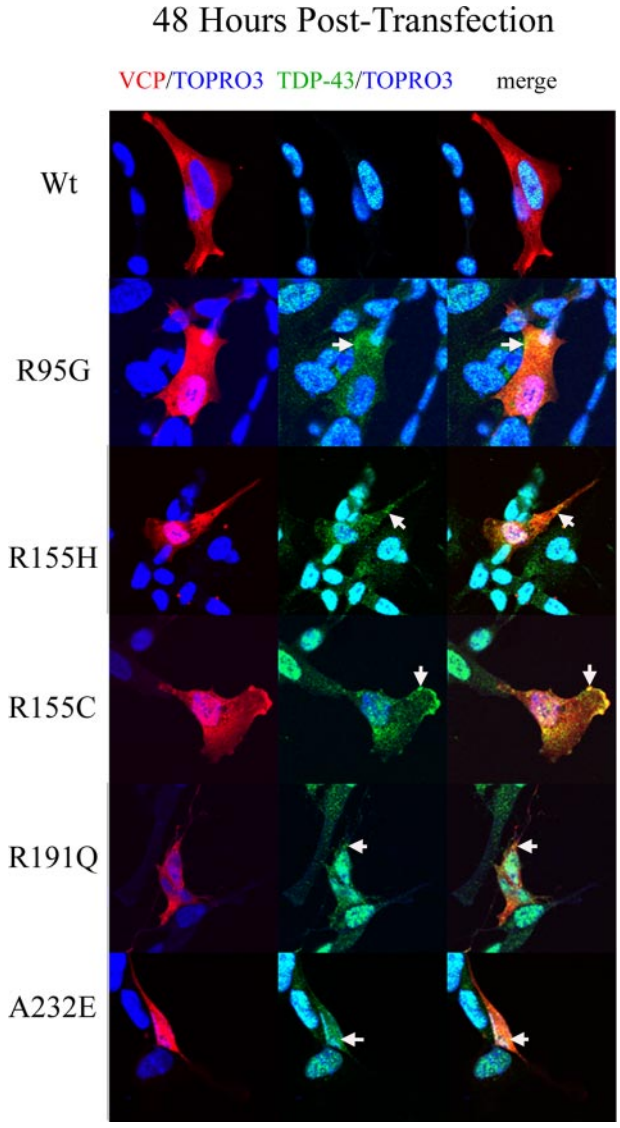

FIGURE 10. **Mutant *VCP* alters endogenous TDP-43 localization 48 h post-transfection.** dsRED-VCP fusion protein (*red*), TDP-43 (*green*), and TOPRO-3 (nuclear marker; *blue*) were visualized by confocal microscopy At 48 h post-transfection. The *arrows* indicate TDP-43 and VCP colocalization in the cytosol (*merge/yellow*).

ER Stress and Unfolded Protein Response Play a Role in VCP Pathogenesis—Because AKT phosphorylation of VCP has been shown to play a role in activation of VCP, we investigated whether induction and/or inhibition of phosphatidylinositol 3-kinase signaling plays a role in the post-translational modification of TDP-43 (21, 53). AKT is induced during differentiation in neuroblastoma cells by the addition of retinoic acid and is inhibited by the phosphoinositide 3-kinase inhibitor LY294002 (*LY*) and untreated SHSY-5Y cells (*5Y*) (Fig. 4*A*; see supplemental Fig. 2) (54). Endogenous VCP (lower band) has been shown previously to be up-regulated in differentiating U937 leukemia and pancreatic ductal adenocarcinoma, but we observed no change in endogenous VCP in retinoic acid-induced differentiated SHSY-5Y cells (Fig. 4*A*, *lower band*) (55, 56). There appeared to be no posttranslational modifications of TDP-43 in mutant *VCP*-expressing cells compared with WT (Fig. 4*A*).

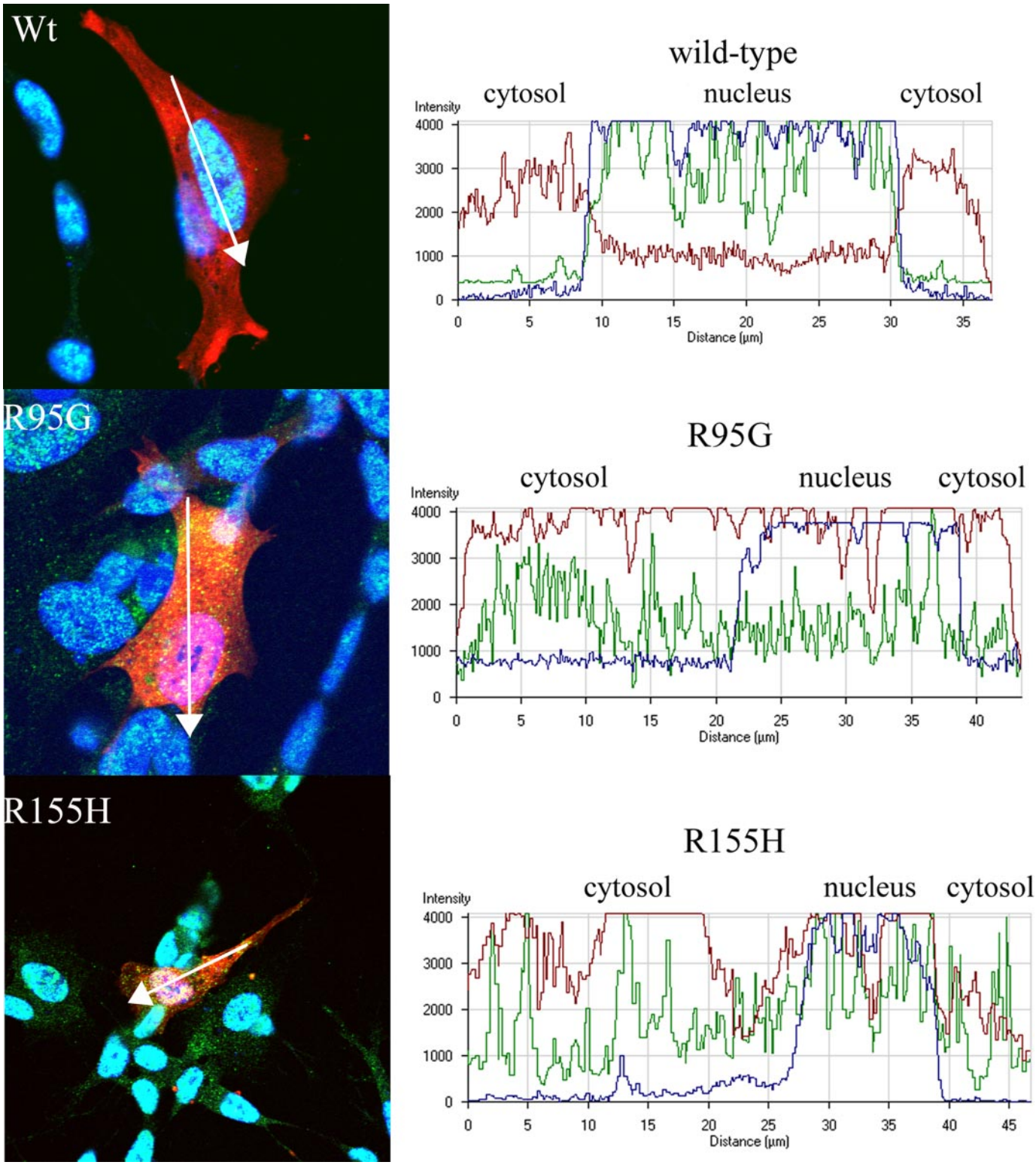

FIGURE 11. **Mutant *VCP* induces TDP-43 distribution to the cytosol 48 h post-transfection.** Wild-type VCP-expressing cells show no change in nuclear distribution of TDP-43. In contrast, VCP R95G and R155H mutants display a relative increase in cytosolic TDP-43. The *graphs* show the intensity distribution profile of dsRED-VCP (*red line*), TDP-43 (*green line*), and TOPRO-3 (nuclear marker; *blue line*) of the *merged image*.

Recently, VCP was shown to have a role in the autophagic clearance of protein aggregates (57), and the loss of endosomal sorting complexes required for transport has been shown to be implicated in the accumulation of TDP-43 (58). In order to investigate the role of aggregation in our overexpression system, we induced autophagy through the phosphatidylinositol 3-kinase inhibitor LY294002 (59). This showed altered localization of TDP-43; there was no difference between the untransfected cells and WT and mutant *VCP* (see supplemental Fig. 2).

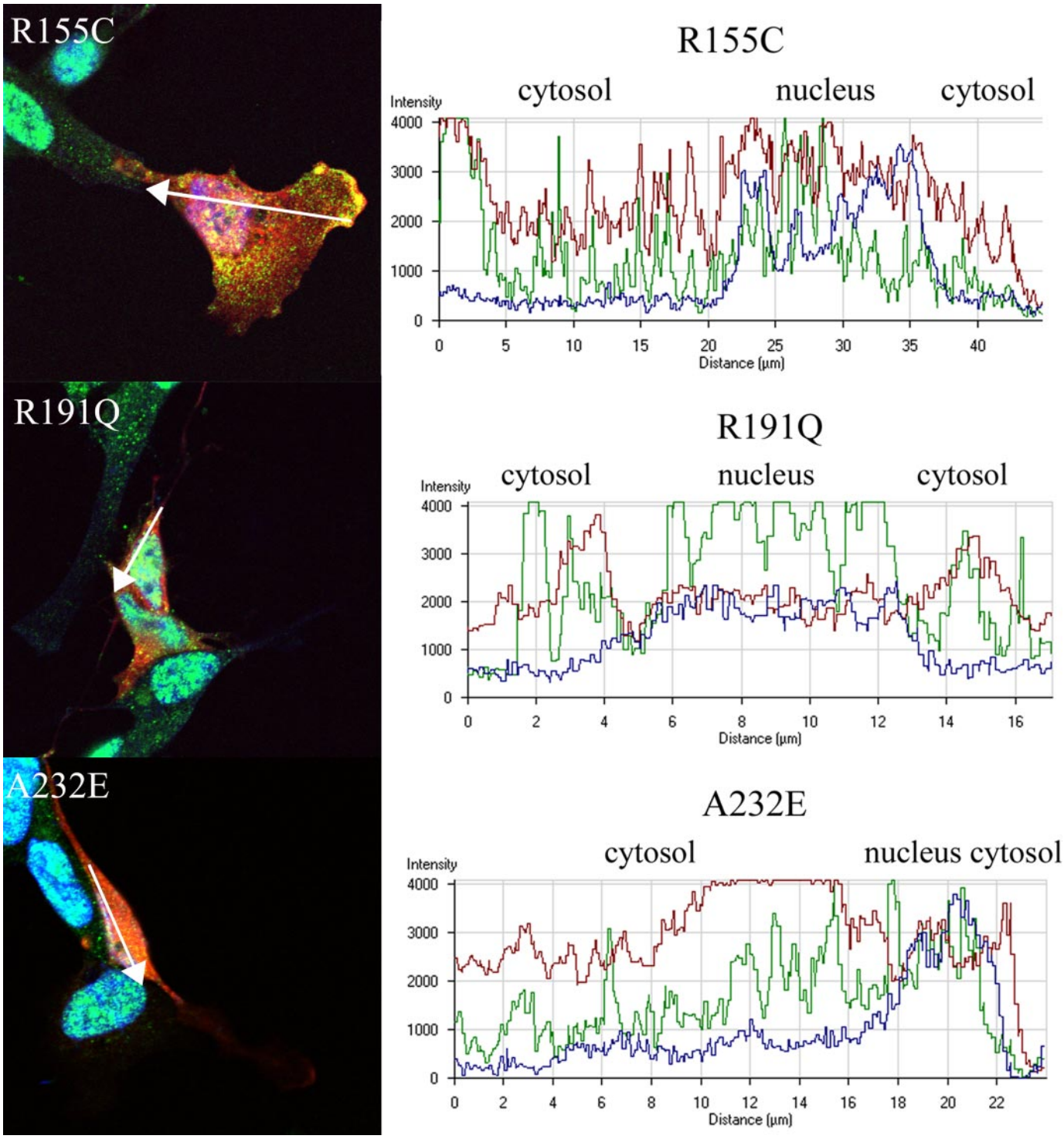

FIGURE 12. **Mutant *VCP* induces TDP-43 distribution from the nucleus to the cytosol 48 h post-transfection.** R155C, R191Q, and A232E mutants display a relative increase in cytosolic TDP-43. The *graphs* show the intensity distribution profile of dsRED-VCP (*red line*), TDP-43 (*green line*), and TOPRO-3 (nuclear marker; *blue line*) of the *merged image*.

GRP78 (BiP), GRP94, CHOP, and XBP1 are activated in response to ER stress (60, 61). GRP78 protein level in untreated cells (5Y) showed no significant difference between nontransfected cells, WT, and all the mutant *VCP* cells, but there was a small increase in protein level when WT transfected cells were compared with R155C, R191Q, and A232E cells (Fig. 4, *A* and *B*) (60). In order to investigate this trend in GRP78 expression, we looked at transcriptional levels by quantitative RT-PCR of GRP78, calreticulin, GRP94, CHOP, and XBP1. We found no significant change in the level of transcription of GRP94, CHOP, or alternative splicing of XBP1 (data not shown). In contrast, the GRP78 transcription level in untreated cells was significantly lower than in WT transfected cells 57.7 ± 2.0 ($p < 0.01$). Compared with WT cells, all *VCP* mutants expressed

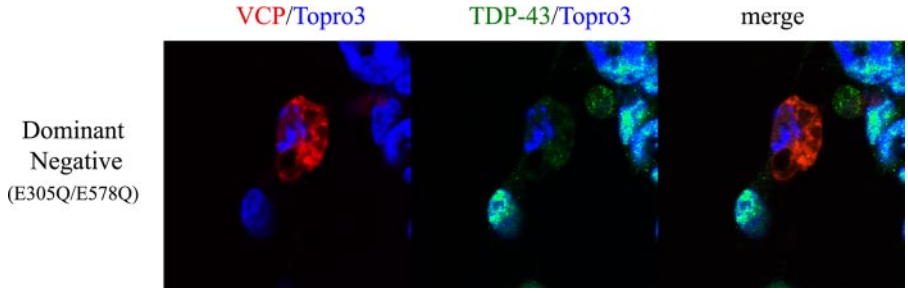

FIGURE 13. **Overexpression of dsRED-VCP E305Q/E578Q (dominant negative) leads to nuclear fragmentation consistent with neuronal cell death at 24 h post-transfection.** There is little to no TDP-43 present either in the nucleus or cytoplasm. dsRED-VCP E305Q/E578Q (dominant negative) (*red*), TDP-43 (*green*) and TOPRO-3 (nuclear marker; *blue*) and visualized by confocal microscopy.

higher levels of GRP78 mRNA than cells overexpressing WT *VCP*: R95G, 42.2 ± 1.1% ($p < 0.05$); R155H, 25.5 ± 8.1% ($p < 0.05$); R155C, 12.7 ± 3.1% ($p < 0.05$); R191Q, 70.6 ± 8.4% ($p < 0.05$); A232E, 74.8 ± 5.6% ($p < 0.001$). The data were obtained from two independent experiments with four replicates. Interestingly, calreticulin displayed no significant change in transcription when WT was compared with mutant *VCP* in untreated cells (data not shown). However, 24 h after the addition of retinoic acid, wild-type VCP-overexpressing cells showed a 237.5 ± 5.3% ($p < 0.001$) increase in calreticulin transcription compared with retinoic acid-treated cells. Wild-type expressing cells compared with mutant *VCP* showed a smaller increase in calreticulin transcription: R95G, 56.5 ± 7.0% ($p < 0.05$); R155H, 141.2 ± 10.3% ($p < 0.001$); R155C, 170.1 ± 1.8% ($p < 0.001$); R191Q, 172.4 ± 7.1% ($p < 0.001$); A232E, 156.6 ± 9.0% ($p < 0.001$). The data were obtained from two independent experiments with four replicates (Fig. 4*D*).

Mutations in VCP Increase Cleaved Caspase Activity—Previously, it has been shown that caspase activity is responsible for post-translational cleavage associated with TDP-43 proteinopathy in FTLD with *GRN* mutation (62). To investigate this pathway in FTLD with *VCP* mutation, we used a colorimetric substrate that can be cleaved by caspase-4 and -9. We demonstrated that cleaved caspase-4 and/or -9 increased significantly in cells overexpressing mutant *VCP* (R95G, 29.0 ± 2.0% ($p < 0.001$); R155H, 30.2 ± 1.5% ($p < 0.001$); R155C, 13.6 ± 1.5% ($p < 0.05$); R191Q, 22.2 ± 2.8% ($p < 0.001$); A232E, 21.0 ± 2.0% ($p < 0.001$; $n = 10$) (Fig. 5*A*) (63). Cleaved caspase-3 activity was also increased in cells expressing mutant VCP: R95G, 25.0 ± 2.3% ($p < 0.001$); R155H, 13.7 ± 2.0% ($p < 0.05$); R155C, 30.5 ± 3.9% ($p < 0.001$); R191Q, 14.7 ± 2.0% ($p < 0.05$); A232E, 40.8 ± 3.5% ($p < 0.001$; $n = 10$) (Fig. 5*B*) (64).

Mutations in VCP Alter Endogenous TDP-43 Localization—To investigate localization and normal distribution of VCP in SHSY-5Y cells, we used confocal microscopy. Distribution of WT VCP was primarily cytosolic, with both ER and Golgi colocalization (Fig. 6). There was no apparent change in the distribution of giantin, a *trans*-Golgi marker, or protein-disulfide isomerase, an ER marker, in cells transfected with mutant *VCP*, indicating that the Golgi and ER do not appear to be fragmented, a feature of some neurodegenerative diseases (Fig. 6) (65). There was no increase in accumulation or change in aggregation of overexpressed WT compared with mutant *VCP*. However, mutant *VCP* was distributed throughout the entire cell compared with WT, which was predominantly localized to the nucleus (Fig. 6).

Since TDP-43 is a predominantly nuclear protein and translocation from the nucleus to the cytoplasm is a signature feature of TDP-43 proteinopathies, including FTLD with *VCP* mutation, we investigated whether overexpression of mutant *VCP* causes a change in localization of endogenous TDP-43 (5, 40, 66). Observations were made at 24 and 48 h time points after transfection. At 24 h after transfection, the WT *VCP*-expressing cells showed no apparent change in distribution or accumulation of TDP-43; there were punctate TDP-43-positive speckles or granules within the cytoplasm in the WT-expressing cells that were less abundant compared with the cells that were not transfected (Fig. 7). VCP and TDP-43 colocalized in both the WT and mutant *VCP*-expressing cells. This TDP-43/VCP colocalization was observed in 65% of the mutant-expressing cells (Fig. 7). Also, in 75% of cells transfected, mutant *VCP* was observed in both the cytoplasm and nucleus. In contrast, in the WT-expressing cells, VCP was predominantly found within the cytoplasm with some punctuate expression in the nucleus (Fig. 7). In order to investigate this distribution, we looked at cytoplasmic and nuclear intensity distribution within the cell using a graphical method (Figs. 8 and 9) (67). As indicated in the intensity line profile, in the WT-transfected cells, TDP-43 was predominantly nuclear, with some cytosolic staining, and where VCP was more abundant. In R95G cells, there was an increase in nuclear localization of VCP that was even more pronounced in R155H, R155C, R191Q, and A232E mutants (Figs. 7–9). TDP-43 distribution within the nucleus was more granular, with some areas being more punctate, most prominently in the R155C-expressing cells (Fig. 9). In untransfected SHSY-5Y cells, the distribution of intensity indicated a normal cytoplasmic distribution of TDP-43 (Fig. 8*B*).

In the viability experiments described above, we observed that cell death occurred 48 h post-transfection (Fig. 3*A*). In order to look at downstream morphological effects and redistribution of TDP-43, we observed these cells 48 h after transfection (Fig. 10). At 48 h post-transfection, WT VCP remained predominantly cytosolic in over 85% of all transfected cells, whereas over 85% of the mutant expressing cells showed a nuclear distribution (Fig. 10). Colocalization of TDP-43 and VCP was apparent in the mutant-expressing cells (Fig. 10). In R95G, R155H, and R155C cells, there was an increase in nuclear colocalization of VCP/TDP-43 as large punctate inclusions (Figs. 11 and 12). Interestingly, A232E mutant-expressing cells displayed a morphologically condensed nucleus, which has been shown previously to be associated with apoptosis (Fig. 12) (68). There was also a punctate cytosolic distribution of TDP-43 that colocalized with VCP (Fig. 11). Nuclear TDP-43 was reduced in mutant VCP cells in comparison with WT cells, as demonstrated by immunoblotting and confocal immunocytochemistry (see supplemental Fig. 3, *A* and B; see Figs. 11 and 12).

VCP was present at a relatively higher intensity within the nucleus of R95G-, R155H-, R155C-, R191Q-, and A234E-expressing cells with very low intensity of wild-type VCP localized to the nucleus (Fig. 12) (see supplemental material for video files showing complete Z-stack distribution of TDP-43 at 48 h post-transfection comparing WT with mutant *VCP* R155H). Overexpression of E305Q/E578Q, a dominant-negative *VCP* mutant, led to nuclear fragmentation consistent with neuronal cell death at 24 h after transfection with little to no TDP-43 present either in the nucleus or cytoplasm (Fig. 13).

TDP-43 and VCP Are Coimmunoprecipitated from SHSY-5Y Cells and Brain—In order to expand our understanding of the colocalization observed in brain and in tissue culture models (Figs. 2 and 8*A*), we investigated whether TDP-43 interacts with VCP using immunoprecipitation methods. We found that TDP-43 and VCP immunoprecipitate together in SHSY-5Y cells and that the *VCP* mutations did not affect the formation of these complexes (Fig. 14*A*). We confirmed that VCP and TDP-43 also coimmunoprecipitate from brain homogenates (Fig 14, *B* and *C*). Interestingly, we found that there was less TDP-43 immunoprecipitated by VCP in a spectrum of TDP-43 proteinopathies (Fig. 14*C*).

DISCUSSION

Loss of VCP function using knockdown experiments results in a decrease in proteasome activity and an increase in ubiquitinated proteins (37). We describe a tissue culture model of FTLD with *VCP* mutation in which mutant transfectants cause a loss of function. Several mechanisms contribute to this loss of function. Mutant *VCP* lowers chymotrypsin cleavage activity of the proteasome and increases soluble ubiquitin, which resembles the accumulation of ubiquitinated proteins, aggregation, change in solubility, and inclusion formation present in the human disease (13, 40). Proteasome dysfunction is implicated in the pathogenesis of Huntington disease, Parkinson disease, motor neuron disease, and other neurodegenerative diseases, but the mode of activation has yet to be elucidated (62, 69, 70). A decrease in proteasome activity not only increases ubiquitinated proteins targeted for degradation but may also affect activation of signaling pathways that are regulated by ubiquitination (43, 71). VCP has been shown to be phosphorylated by AKT and also has a role in ubiquitination of IκBα activating the NF-κB cell survival pathway (21, 35, 53). Modulation of VCP expression has been implicated in cancer and apoptotic pathways (56, 72). Proteasome malfunction has been shown to activate the caspase cascade and, eventually, apoptotic cell death (69). Activation of ER stress and the unfolded protein response has been shown previously to induce the caspase cascade (63, 73, 74). We describe a specific induction of ER stress involving an increase in the molecular chaperone GRP78. A unique function of VCP in retinoic acid-induced differentiation of neuroblastoma cells is to affect the transcriptional level of calreticulin. This protein monitors unfolded glycoproteins, which may lead to an accumulation of these substrates not targeted correctly through ERAD to the proteasome (Fig. 4*C*) (75–78). Although mutations in *VCP* have been shown previously to be defective in targeting specific substrates through ERAD, the specific mechanism leading to this defect has not been eluci-

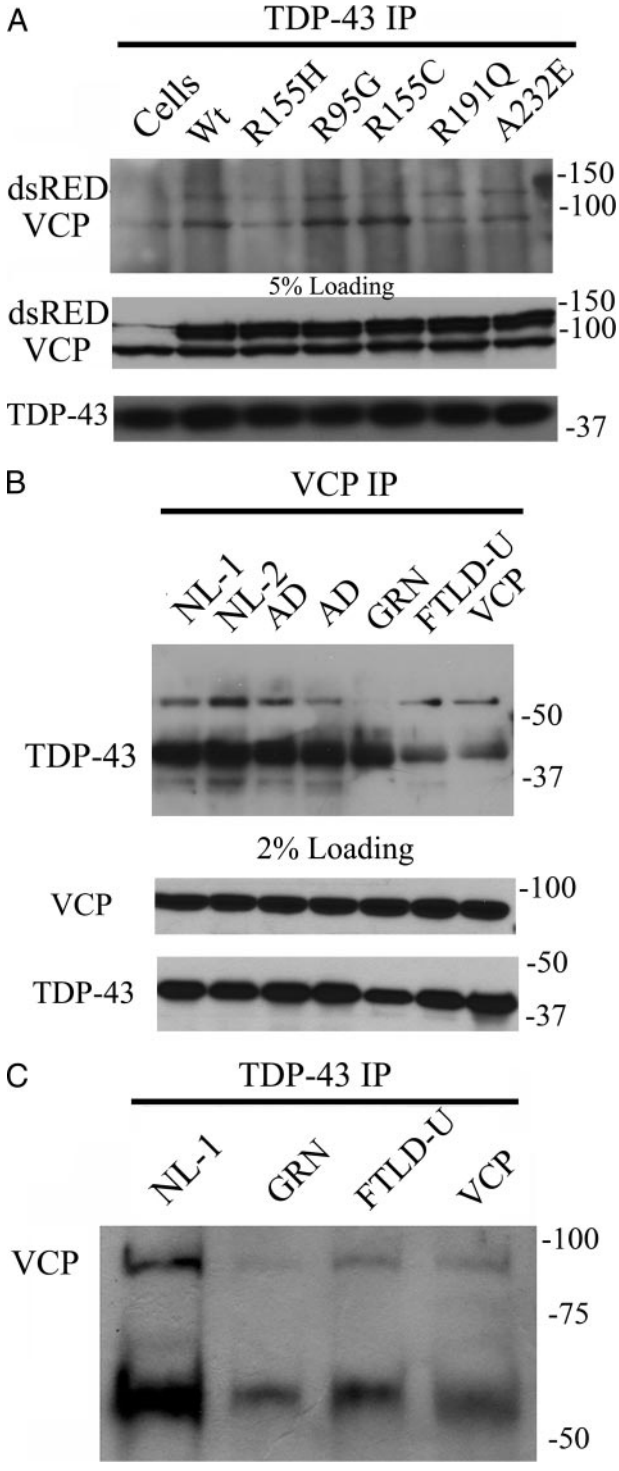

FIGURE 14. **TDP-43 complexes with VCP in co-immunoprecipitation assays in both SHSY-5Y cells and human brain.** *A*, TDP-43 immunoprecipitation (*IP*) in VCP-transfected SHSY-5Y cells probed with anti-VCP (*top*) and 5% loading control (*bottom*). *B*, VCP immunoprecipitation in high salt (*HS*) fraction of human brain probed with anti-TDP-43. Samples were immunoprecipitated with VCP: normal adult control cases (*NL-1* and *NL-2*); Alzheimer disease (*AD*); familial FTLD-U with *GRN* A9D mutation (*GRN*); sporadic (*FTLD-U*); and FTLD-U with the *VCP* R155H mutation (*VCP*) (*top*) and 2% loading control (*bottom*). *C*, TDP-43 immunoprecipitation in HS of human brain probed with anti-VCP: age-matched control (*NL-1*); familial FTLD-U with *GRN* A9D mutation (*GRN*); sporadic (*FTLD-U*); and FTLD-U with *VCP* R155H mutation (*VCP*).

dated, and the relationship between VCP and calreticulin needs further investigation (50).

In the SHSY-5Y model system, the spatial relocalization of TDP-43 in cells expressing mutant *VCP* resembles the altered localization of TDP-43 with KCl-induced neuronal stress (79). Although the predominant pathology in FTLD with *VCP* mutation is TDP-43 proteinopathy in the form of NIIs, we demonstrate in this tissue culture model that this change in localization of TDP-43 is present before cell death. Also, the mutant *VCP* localizes to the nucleus and cytosol, whereas WT VCP was predominantly cytosolic, which recapitulates features of the human disease (2).

In summary, we describe an *in vitro* model of FTLD with *VCP* mutation. Transfected mutant VCP in neuroblastoma cells induced cell death and caused relocation of TDP-43. To determine potential mechanisms of neurodegeneration, we report a novel interaction between TDP-43 and VCP in tissue culture that is also detected in brain. This interaction requires further investigation, but it suggests that TDP-43 may be a substrate targeted to the proteasome or may modulate VCP function as a cofactor. The ability of TDP-43 to bind single-stranded DNA may indicate a role for VCP targeted to sites of DNA repair (17, 20). Elucidating the relationship of the interaction between TDP-43 and VCP will provide further insights into the pathogenesis of this TDP-43 proteinopathy (21, 35, 53, 66, 80) and provide novel targets for therapeutic intervention.

Acknowledgments—We thank Dr. John C. Morris and the clinical, genetic, pathology, and technical staff of the Washington University Alzheimer's Disease Research Center for making information and tissue samples available for this study, and we thank the families of patients whose generosity made this research possible.

REFERENCES

1. Bird, T., Knopman, D., VanSwieten, J., Rosso, S., Feldman, H., Tanabe, H., Graff-Raford, N., Geschwind, D., Verpillat, P., and Hutton, M. (2003) *Ann. Neurol.* **54,** Suppl. 5, 29–31
2. Cairns, N. J., Bigio, E. H., Mackenzie, I. R., Neumann, M., Lee, V. M., Hatanpaa, K. J., White, C. L., III, Schneider, J. A., Grinberg, L. T., Halliday, G., Duyckaerts, C., Lowe, J. S., Holm, I. E., Tolnay, M., Okamoto, K., Yokoo, H., Murayama, S., Woulfe, J., Munoz, D. G., Dickson, D. W., Ince, P. G., Trojanowski, J. Q., and Mann, D. M. (2007) *Acta Neuropathol.* **114,** 5–22
3. Cairns, N. J., Neumann, M., Bigio, E. H., Holm, I. E., Troost, D., Hatanpaa, K. J., Foong, C., White, C. L., III, Schneider, J. A., Kretzschmar, H. A., Carter, D., Taylor-Reinwald, L., Paulsmeyer, K., Strider, J., Gitcho, M., Goate, A. M., Morris, J. C., Mishra, M., Kwong, L. K., Stieber, A., Xu, Y., Forman, M. S., Trojanowski, J. Q., Lee, V. M., and Mackenzie, I. R. (2007) *Am. J. Pathol.* **171,** 227–240
4. Bersano, A., Del Bo, R., Lamperti, C., Ghezzi, S., Fagiolari, G., Fortunato, F., Ballabio, E., Moggio, M., Candelise, L., Galimberti, D., Virgilio, R., Lanfranconi, S., Torrente, Y., Carpo, M., Bresolin, N., Comi, G. P., and Corti, S. (2007) *Neurobiol. Aging* 10.1016/jneurobiolaging.2007.08.009
5. Guyant-Maréchal, L., Laquerriére, A., Duyckaerts, C., Dumanchin, C., Bou, J., Dugny, F., Le, B. I., Frébourg, T., Hannequin, D., and Campion, D. (2006) *Neurology* **67,** 644–651
6. Haubenberger, D., Bittner, R. E., Rauch-Shorny, S., Zimprich, F., Mannhalter, C., Wagner, L., Mineva, I., Vass, K., Auff, E., and Zimprich, A. (2005) *Neurology* **65,** 1304–1305
7. Kimonis, V. E., and Watts, G. D. (2005) *Alzheimer Dis. Assoc. Disord.* **19,** Suppl. 1, 44–47
8. Kovach, M. J., Waggoner, B., Leal, S. M., Gelber, D., Khardori, R., Levenstien, M. A., Shanks, C. A., Gregg, G., Al Lozi, M. T., Miller, T., Rakowicz, W., Lopate, G., Florence, J., Glosser, G., Simmons, Z., Morris, J. C., Whyte, M. P., Pestronk, A., and Kimonis, V. E. (2001) *Mol. Genet. Metab.* **74,** 458–475
9. Watts, G. D., Wymer, J., Kovach, M. J., Mehta, S. G., Mumm, S., Darvish, D., Pestronk, A., Whyte, M. P., and Kimonis, V. E. (2004) *Nat. Genet.* **36,** 377–381
10. Watts, G. D., Thomasova, D., Ramdeen, S. K., Fulchiero, E. C., Mehta, S. G., Drachman, D. A., Weihl, C. C., Jamrozik, Z., Kwiecinski, H., Kaminska, A., and Kimonis, V. E. (2007) *Clin. Genet.* **72,** 420–426
11. Daroszewska, A., and Ralston, S. H. (2006) *Nat. Clin. Pract. Rheumatol.* **2,** 270–277
12. Hubbers, C. U., Clemen, C. S., Kesper, K., Boddrich, A., Hofmann, A., Kamarainen, O., Tolksdorf, K., Stumpf, M., Reichelt, J., Roth, U., Krause, S., Watts, G., Kimonis, V., Wattjes, M. P., Reimann, J., Thal, D. R., Biermann, K., Evert, B. O., Lochmuller, H., Wanker, E. E., Schoser, B. G., Noegel, A. A., and Schroder, R. (2007) *Brain* **130,** 381–393
13. Forman, M. S., Mackenzie, I. R., Cairns, N. J., Swanson, E., Boyer, P. J., Drachman, D. A., Jhaveri, B. S., Karlawish, J. H., Pestronk, A., Smith, T. W., Tu, P. H., Watts, G. D., Markesbery, W. R., Smith, C. D., and Kimonis, V. E. (2006) *J. Neuropathol. Exp. Neurol.* **65,** 571–581
14. Davidson, Y., Kelley, T., Mackenzie, I. R., Pickering-Brown, S., Du, P. D., Neary, D., Snowden, J. S., and Mann, D. M. (2007) *Acta Neuropathol.* **113,** 521–533
15. Neumann, M., Sampathu, D. M., Kwong, L. K., Truax, A. C., Micsenyi, M. C., Chou, T. T., Bruce, J., Schuck, T., Grossman, M., Clark, C. M., McCluskey, L. F., Miller, B. L., Masliah, E., Mackenzie, I. R., Feldman, H., Feiden, W., Kretzschmar, H. A., Trojanowski, J. Q., and Lee, V. M. (2006) *Science* **314,** 130–133
16. Neumann, M., Mackenzie, I. R., Cairns, N. J., Boyer, P. J., Markesbery, W. R., Smith, C. D., Taylor, J. P., Kretzschmar, H. A., Kimonis, V. E., and Forman, M. S. (2007) *J. Neuropathol. Exp. Neurol.* **66,** 152–157
17. Zhang, H., Wang, Q., Kajino, K., and Greene, M. I. (2000) *DNA Cell Biol.* **19,** 253–263
18. Shiozawa, K., Maita, N., Tomii, K., Seto, A., Goda, N., Akiyama, Y., Shimizu, T., Shirakawa, M., and Hiroaki, H. (2004) *J. Biol. Chem.* **279,** 50060–50068
19. Shiozawa, K., Goda, N., Shimizu, T., Mizuguchi, K., Kondo, N., Shimozawa, N., Shirakawa, M., and Hiroaki, H. (2006) *FEBS J.* **273,** 4959–4971
20. Livingstone, M., Ruan, H., Weiner, J., Clauser, K. R., Strack, P., Jin, S., Williams, A., Greulich, H., Gardner, J., Venere, M., Mochan, T. A., DiTullio, R. A., Jr., Moravcevic, K., Gorgoulis, V. G., Burkhardt, A., and Halazonetis, T. D. (2005) *Cancer Res.* **65,** 7533–7540
21. Vandermoere, F., Yazidi-Belkoura, I., Slomianny, C., Demont, Y., Bidaux, G., Adriaenssens, E., Lemoine, J., and Hondermarck, H. (2006) *J. Biol. Chem.* **281,** 14307–14313
22. Hui, L., Pei, D. S., Zhang, Q. G., Guan, Q. H., and Zhang, G. Y. (2005) *Brain Res.* **1052,** 1–9
23. Alzayady, K. J., Panning, M. M., Kelley, G. G., and Wojcikiewicz, R. J. (2005) *J. Biol. Chem.* **280,** 34530–34537
24. Lavoie, C., Chevet, E., Roy, L., Tonks, N. K., Fazel, A., Posner, B. I., Paiement, J., and Bergeron, J. J. (2000) *Proc. Natl. Acad. Sci. U. S. A.* **97,** 13637–13642
25. Dreveny, I., Kondo, H., Uchiyama, K., Shaw, A., Zhang, X., and Freemont, P. S. (2004) *EMBO J.* **23,** 1030–1039
26. Kano, F., Tanaka, A. R., Yamauchi, S., Kondo, H., and Murata, M. (2004) *Mol. Biol. Cell* **15,** 4289–4298
27. Kano, F., Kondo, H., Yamamoto, A., Tanaka, A. R., Hosokawa, N., Nagata, K., and Murata, M. (2005) *Genes Cells* **10,** 333–344
28. Ballar, P., Shen, Y., Yang, H., and Fang, S. (2006) *J. Biol. Chem.* **281,** 35359–35368
29. Miyachi, K., Hirano, Y., Horigome, T., Mimori, T., Miyakawa, H., Onozuka, Y., Shibata, M., Hirakata, M., Suwa, A., Hosaka, H., Matsushima, S., Komatsu, T., Matsushima, H., Hankins, R. W., and Fritzler, M. J. (2004) *Clin. Exp. Immunol.* **136,** 568–573
30. Pye, V. E., Beuron, F., Keetch, C. A., McKeown, C., Robinson, C. V., Meyer,

H. H., Zhang, X., and Freemont, P. S. (2007) *Proc. Natl. Acad. Sci. U. S. A.* **104,** 467–472
31. Partridge, J. J., Lopreiato, J. O., Jr., Latterich, M., and Indig, F. E. (2003) *Mol. Biol. Cell* **14,** 4221–4229
32. DeLaBarre, B., Christianson, J. C., Kopito, R. R., and Brunger, A. T. (2006) *Mol. Cell* **22,** 451–462
33. McCracken, A. A., and Brodsky, J. L. (1996) *J. Cell Biol.* **132,** 291–298
34. Schmitz, A., and Herzog, V. (2004) *Eur. J. Cell Biol.* **83,** 501–509
35. Asai, T., Tomita, Y., Nakatsuka, S., Hoshida, Y., Myoui, A., Yoshikawa, H., and Aozasa, K. (2002) *Jpn. J. Cancer Res.* **93,** 296–304
36. Nowis, D., McConnell, E., and Wojcik, C. (2006) *Exp. Cell Res.* **312,** 2921–2932
37. Wojcik, C., Rowicka, M., Kudlicki, A., Nowis, D., McConnell, E., Kujawa, M., and DeMartino, G. N. (2006) *Mol. Biol. Cell* **17,** 4606–4618
38. Mukherjee, O., Pastor, P., Cairns, N. J., Chakraverty, S., Kauwe, J. S., Shears, S., Behrens, M. I., Budde, J., Hinrichs, A. L., Norton, J., Levitch, D., Taylor-Reinwald, L., Gitcho, M., Tu, P. H., Tenenholz, G. L., Liscic, R. M., Armendariz, J., Morris, J. C., and Goate, A. M. (2006) *Ann. Neurol.* **60,** 314–322
39. Sampathu, D. M., Neumann, M., Kwong, L. K., Chou, T. T., Micsenyi, M., Truax, A., Bruce, J., Grossman, M., Trojanowski, J. Q., and Lee, V. M. (2006) *Am. J. Pathol.* **169,** 1343–1352
40. Gitcho, M. A., Baloh, R. H., Chakraverty, S., Mayo, K., Norton, J. B., Levitch, D., Hatanpaa, K. J., White, C. L., III, Bigio, E. H., Caselli, R., Baker, M., Al Lozi, M. T., Morris, J. C., Pestronk, A., Rademakers, R., Goate, A. M., and Cairns, N. J. (2008) *Ann. Neurol.* **63,** 535–538
41. Mukherjee, O., Wang, J., Gitcho, M., Chakraverty, S., Taylor-Reinwald, L., Shears, S., Kauwe, J. S., Norton, J., Levitch, D., Bigio, E. H., Hatanpaa, K. J., White, C. L., Morris, J. C., Cairns, N. J., and Goate, A. (2008) *Hum. Mutat.* **29,** 512–521
42. Bursztajn, S., Feng, J. J., Nanda, A., and Berman, S. A. (2001) *Brain Res. Mol. Brain Res.* **91,** 57–72
43. Li, X., Yang, D., Li, L., Peng, C., Chen, S., and Le, W. (2007) *Neurochem. Int.* **50,** 959–965
44. Qiu, J. H., Asai, A., Chi, S., Saito, N., Hamada, H., and Kirino, T. (2000) *J. Neurosci.* **20,** 259–265
45. Snider, B. J., Tee, L. Y., Canzoniero, L. M., Babcock, D. J., and Choi, D. W. (2002) *Eur. J. Neurosci.* **15,** 419–428
46. Muller, P. Y., Janovjak, H., Miserez, A. R., and Dobbie, Z. (2002) *BioTechniques* **32,** 1372–1379
47. Nilbratt, M., Friberg, L., Mousavi, M., Marutle, A., and Nordberg, A. (2007) *J. Neurosci. Res.* **85,** 504–514
48. Christophersen, N. S., Meijer, X., Jorgensen, J. R., Englund, U., Gronborg, M., Seiger, A., Brundin, P., and Wahlberg, L. U. (2006) *Brain Res. Bull.* **70,** 457–466
49. Aravindan, N., Madhusoodhanan, R., Natarajan, M., and Herman, T. S. (2008) *Mol. Cell Biochem.* **310,** 167–179
50. Weihl, C. C., Dalal, S., Pestronk, A., and Hanson, P. I. (2006) *Hum. Mol. Genet.* **15,** 189–199
51. Shenkman, M., Tolchinsky, S., and Lederkremer, G. Z. (2007) *Cell Stress Chaperones* **12,** 373–383
52. Shenkman, M., Tolchinsky, S., Kondratyev, M., and Lederkremer, G. Z. (2007) *Biochem. J.* **404,** 509–516
53. Klein, J. B., Barati, M. T., Wu, R., Gozal, D., Sachleben, L. R., Jr., Kausar, H., Trent, J. O., Gozal, E., and Rane, M. J. (2005) *J. Biol. Chem.* **280,** 31870–31881
54. Lopez-Carballo, G., Moreno, L., Masia, S., Perez, P., and Barettino, D. (2002) *J. Biol. Chem.* **277,** 25297–25304
55. Bertram, C., von Neuhoff, N., Skawran, B., Steinemann, D., Schlegelberger, B., and Hass, R. (2008) *BMC Cell Biol.* **9,** 1–16
56. Yamamoto, S., Tomita, Y., Hoshida, Y., Nagano, H., Dono, K., Umeshita, K., Sakon, M., Ishikawa, O., Ohigashi, H., Nakamori, S., Monden, M., and Aozasa, K. (2004) *Ann. Surg. Oncol.* **11,** 165–172
57. Ju, J. S., Miller, S. E., Hanson, P. I., and Weihl, C. C. (2008) *J. Biol. Chem.*
58. Filimonenko, M., Stuffers, S., Raiborg, C., Yamamoto, A., Malerod, L., Fisher, E. M., Isaacs, A., Brech, A., Stenmark, H., and Simonsen, A. (2007) *J. Cell Biol.* **179,** 485–500
59. Xing, C., Zhu, B., Liu, H., Yao, H., and Zhang, L. (2008) *Acta Biochim. Biophys. Sin.* **40,** 194–201
60. Kondratyev, M., Avezov, E., Shenkman, M., Groisman, B., and Lederkremer, G. Z. (2007) *Exp. Cell Res.* **313,** 3395–3407
61. Lass, A., Kujawa, M., McConnell, E., Paton, A. W., Paton, J. C., and Wojcik, C. (2008) *Int. J. Biochem. Cell Biol.* **40,** 2865–2879
62. Zhang, Y. J., Xu, Y. F., Dickey, C. A., Buratti, E., Baralle, F., Bailey, R., Pickering-Brown, S., Dickson, D., and Petrucelli, L. (2007) *J. Neurosci.* **27,** 10530–10534
63. Kim, S. J., Zhang, Z., Hitomi, E., Lee, Y. C., and Mukherjee, A. B. (2006) *Hum. Mol. Genet.* **15,** 1826–1834
64. King, T. D., Bijur, G. N., and Jope, R. S. (2001) *Brain Res.* **919,** 106–114
65. Nakagomi, S., Barsoum, M. J., Bossy-Wetzel, E., Sutterlin, C., Malhotra, V., and Lipton, S. A. (2008) *Neurobiol. Dis.* **29,** 221–231
66. Neumann, M., Kwong, L. K., Truax, A. C., Vanmassenhove, B., Kretzschmar, H. A., Van Deerlin, V. M., Clark, C. M., Grossman, M., Miller, B. L., Trojanowski, J. Q., and Lee, V. M. (2007) *J. Neuropathol. Exp. Neurol.* **66,** 177–183
67. Beatty, W. L. (2008) *Infect. Immun.* **76,** 2872–2881
68. Zhivotosky, B., and Orrenius, S. (2001) *Current Protocols in Cell Biology*, Unit 18.3, John Wiley & Sons, Hoboken, NJ
69. Mishra, M., Paunesku, T., Woloschak, G. E., Siddique, T., Zhu, L. J., Lin, S., Greco, K., and Bigio, E. H. (2007) *Acta Neuropathol.* **114,** 81–94
70. Wang, J., Wang, C. E., Orr, A., Tydlacka, S., Li, S. H., and Li, X. J. (2008) *J. Cell Biol.* **180,** 1177–1189
71. Peng, Y., Liu, X., and Schoenberg, D. R. (2008) *Mol. Biol. Cell* **19,** 546–552
72. Zucchini, C., Rocchi, A., Manara, M. C., De Sanctis, P., Capanni, C., Bianchini, M., Carinci, P., Scotlandi, K., and Valvassori, L. (2008) *Int. J. Oncol.* **32,** 17–31
73. Meares, G. P., Zmijewska, A. A., and Jope, R. S. (2008) *Cell. Signal.* **20,** 347–358
74. Medigeshi, G. R., Lancaster, A. M., Hirsch, A. J., Briese, T., Lipkin, W. I., Defilippis, V., Fruh, K., Mason, P. W., Nikolich-Zugich, J., and Nelson, J. A. (2007) *J. Virol.* **81,** 10849–10860
75. Ito, M., Onuki, R., Bando, Y., Tohyama, M., and Sugiyama, Y. (2007) *Biochem. Biophys. Res. Commun.* **360,** 615–620
76. Langer, R., Feith, M., Siewert, J. R., Wester, H. J., and Hoefler, H. (2008) *BMC Cancer* **8,** 1–9
77. Hebert, D. N., Foellmer, B., and Helenius, A. (1995) *Cell* **81,** 425–433
78. Okuda-Shimizu, Y., and Hendershot, L. M. (2007) *Mol. Cell* **28,** 544–554
79. Wang, I. F., Wu, L. S., Chang, H. Y., and Shen, C. K. (2008) *J. Neurochem.* **105,** 797–806
80. Arai, T., Hasegawa, M., Akiyama, H., Ikeda, K., Nonaka, T., Mori, H., Mann, D., Tsuchiya, K., Yoshida, M., Hashizume, Y., and Oda, T. (2006) *Biochem. Biophys. Res. Commun.* **351,** 602–611
81. Gitcho, M. A., Strider, J., Carter, D., Taylor-Reinwald, L., Forman, M. S., Goate, A. M., and Cairns, N. J. (2008) *6th International Conference on Frontotemporal Dementias, Rotterdam, The Netherlands, September 6, 2008* (abstr.)